



Multifunctional homoleptic iridium(III) dendrimers towards solution-processed nondoped electrophosphorescence with low efficiency roll-off

Minrong Zhu^a, Yanhu Li^b, Jingsheng Miao^b, Bei Jiang^a, Chuluo Yang^{a,*}, Hongbin Wu^{b,*}, Jingui Qin^a, Yong Cao^b

^a Hubei Collaborative Innovation Center for Advanced Organic Chemical Materials, Hubei Key Lab on Organic and Polymeric Optoelectronic Materials, Department of Chemistry, Wuhan University, Wuhan 430072, People's Republic of China

^b Institute of Polymer Optoelectronic Materials and Devices, State Key Laboratory of Luminescent Materials and Devices, South China University of Technology, Guangzhou 510640, People's Republic of China

ARTICLE INFO

Article history:

Received 23 October 2013

Received in revised form 2 April 2014

Accepted 8 April 2014

Available online 24 April 2014

Keywords:

Iridium complex

Electrophosphorescence

Charge transport

Dendrimer

ABSTRACT

A series of new iridium dendrimers comprised of bifunctional charge transport peripheral groups have been designed and facilely synthesized. The relationship between the structures and their photophysical, electrochemical and electrophosphorescent performances is investigated. Through the incorporation of rigid electron-transporting phosphine oxide groups and/or hole-transporting arylamine units, the new complexes all have good thermal stabilities with high glass-transition temperature up to 284 °C. Besides, the peripheries sufficiently shield the emissive core from the intermolecular interactions and prevent luminance quenching in neat films. Solution-processed phosphorescent organic light-emitting device (PhOLED) based on bipolar phosphor **2** as neat emitter achieves a maximum current efficiency of 12.4 cd A⁻¹ with Commission Internationale de l'Eclairage coordinates of (0.57, 0.42), and the value remains at 11.5 cd A⁻¹ at a practical luminance of 1000 cd m⁻². This low roll-off can be attributed to the bipolar nature of the emitter. This indicates that rational incorporation of charge-transporting moieties into the sphere of iridium(III) core is a simple and effective approach to develop efficient host-free phosphors for solution-processable nondoped PhOLEDs.

© 2014 Elsevier B.V. All rights reserved.

1. Introduction

During the past decade, organic light-emitting diodes (OLEDs) have emerged as competitive candidates for solid-state lighting sources and full-color flat-panel displays [1]. Endowed with the capability to harvest both singlet and triplet excitons, phosphorescent organic light-emitting diodes (PhOLEDs) with transition metal complexes as luminescent materials have attracted

considerable interests because of the demonstrated potential for achieving unity internal quantum efficiency [2]. Given this, the search for stable and efficient phosphorescent emitters covering the entire visible light spectrum is particularly crucial for the commercialization of OLEDs [3]. Since it could act as the complementary color of the blue one to realize high-performance white light emission, the development of efficient orange phosphors has attracted great attention [4].

Till now, most of the efficient PhOLEDs have been fabricated through vacuum thermal evaporation in multilayer configurations [5]. But the layer-by-layer deposition technique allowing for complicated device structures to

* Corresponding authors. Tel.: +86 27 68756101.

E-mail addresses: clyang@whu.edu.cn (C. Yang), hbwu@scut.edu.cn (H. Wu).

achieve high performance is a rather costly process. Tedious and complicated device fabrication processes are too far cost-effective to compete with other contemporary flat-display technologies. To simplify the device structure, many multifunctional materials possessing luminescent and charge injection/transporting characteristics have been developed [6]. Though numerous efforts have been carried out to improve the performance of the solution-processed PhOLEDs, their efficiencies are still far behind the vacuum-evaporated devices [7].

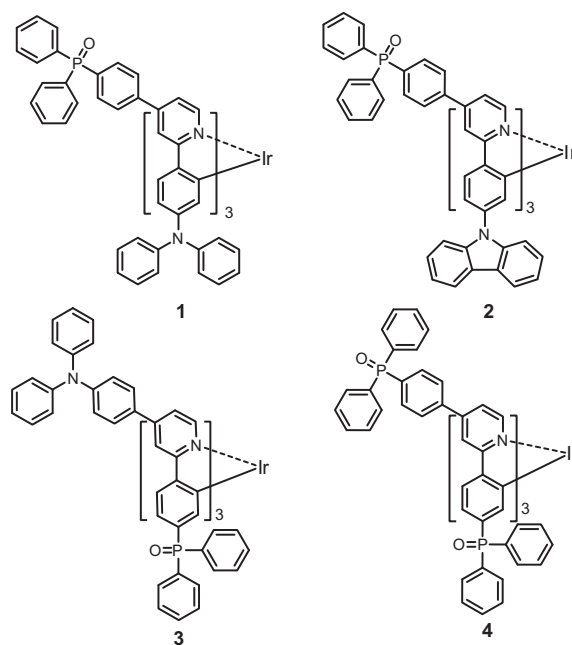
Recently, several groups have been interested in integration of functional units with charge injection and transporting characters into the organic ligands to generate small-molecule or dendritic heavy metal emitters [8]. We have developed a series of triphenylamine-based iridium dendrimers for highly efficient solution-processed electrophosphorescence [9]. Bearing excellent hole-transporting ability, the outer triphenylamine units not only act as good spacers isolating the iridium core but also participate straightforwardly in charge injection, transport and energy transfer. We have demonstrated that the first-generation of the current Ir dendritic array is structurally enough for solution-processable host-free phosphors. Up to now, most of the functional iridium complexes and/or dendrimers reported have been constructed from hole-type arylamine groups or polyphenylene dendrons [10]. Generally, electron mobilities of organic materials are usually two or three orders of magnitude lower than hole mobilities, which would lead to reduced device efficiency and lifetime due to poor carrier balance and an accumulation of positive charge in the recombination zone [11].

To address this issue, we have designed and synthesized four first-generation iridium dendrimers (Scheme 1) featured with electron-transporting phosphine oxide groups and/or hole-transporting arylamine units to facilitate charge injection/transport, and explored their applications as nondoped emitters for solution-processed electrophosphorescence. Phosphine oxide derivatives have been the subject of electron-transport materials for optoelectronic devices [12]. We anticipate that the charge balance of the self-host iridium dendrimers could be manipulated at molecular level through the integration of the electron-donor and -acceptor.

2. Results and discussion

2.1. Synthesis and characterization

Scheme 2 illustrates the synthesis of the new first-generation iridium(III) dendrimers **1–4**. For **L1**, **L2** and **L3**, different charge-transporting aryl groups were attached to the 2,4-dibromopyridine through stepwise Suzuki–Miyaura cross-coupling reactions to form unsymmetrically functionalized ligands [13]. **L4** bearing two electron-withdrawing aryl phosphine oxide was prepared in one step using the same coupling reaction. The preparation of homoleptic complexes was accomplished with a procedure previously reported by us, which involved treating $\text{Ir}(\text{acac})_3$ ($\text{acac} = 2,4\text{-pentanedionate}$) with 3.2 equiv of free ligand in glycerol mixed with 2-(2-methoxyethoxy)ethanol



Scheme 1. The chemical structures of complexes **1–4**.

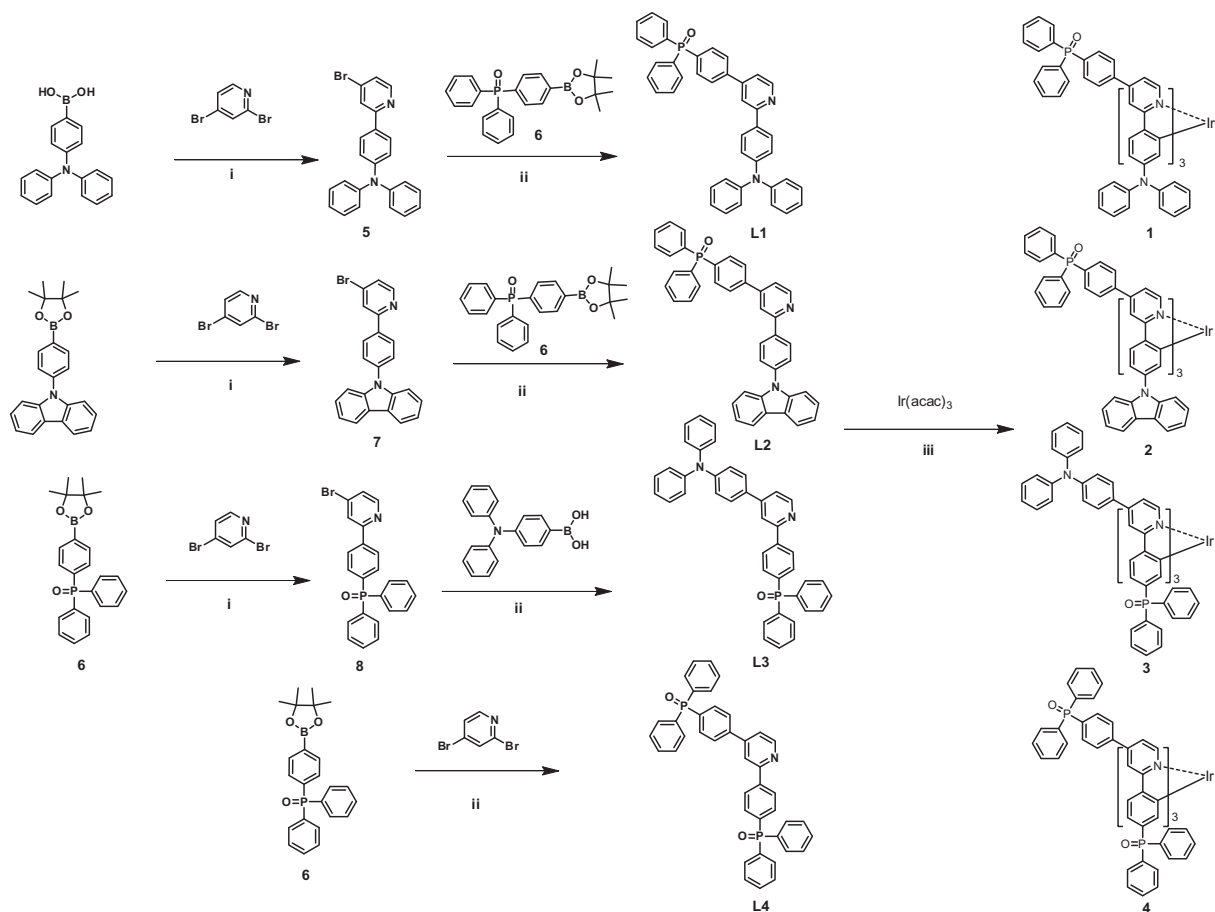
and *o*-dichlorobenzene proportionally at 230 °C. The chemical structures of the iridium complexes were verified by ^1H NMR, ^{13}C NMR spectroscopy, and matrix-assisted laser desorption–ionization time-of-flight (MALDI-TOF) mass spectrometry, and elemental analysis.

2.2. Thermal properties

The thermal properties of the new phosphors were investigated by using differential scanning calorimetry (DSC) and thermogravimetric analysis (TGA). With molecular weights above 1900 g mol^{-1} , the four phosphors show thermal-decomposition temperatures (T_d , corresponding to 5% weight loss, Fig. 1) around 500 °C, which are much higher than those of small-molecule phosphors $\text{Ir}(\text{ppy})_3$ (413 °C) and $\text{Ir}(\text{piq})_3$ (384 °C) [14]. Furthermore, they all exhibit very high glass-transition temperatures (T_g) in the ranges from 246 °C to 284 °C. Among them, complex **4** has the highest T_g value (284 °C) due to the presence of two bulky and rigid phosphine oxide groups, which is consistent to the findings that the presence of arylphosphine oxide moieties incorporated into polymers imparts high thermal stability [15]. Compared with those of **1** and **3** bearing triphenylamine unit, **2** with carbazole as electron-donor reveals higher T_g value since carbazole is more rigid than triphenylamine [16]. The excellent thermal properties of the phosphorescent emitters should favor the morphological stability of thin films in nondoped electroluminescent devices.

2.3. Photophysical properties

The absorption and PL spectra of the complexes recorded in toluene and films are presented in Fig. 2. The intense absorptions in the range of 340–380 nm can be



Scheme 2. Synthetic routes of bipolar Ir(III) complexes. Reagents and conditions: (i) Pd(PPh₃)₄, 2 M Na₂CO₃, THF, reflux, 48 h; (ii) Pd(PPh₃)₄, 2 M Na₂CO₃, toluene, ethanol, reflux, 48 h; (iii) Ir(acac)₃, *o*-dichlorobenzene, 2-(2-methoxyethoxy)ethanol, glycerol, 230 °C, 36 h.

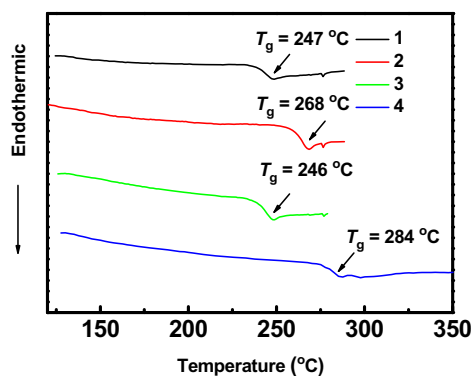


Fig. 1. DSC traces of 1–4 recorded at a heating rate of 10 °C min⁻¹.

assigned to the spin-allowed π – π^* transitions of cyclo-metalating ligands. The weak absorption shoulders in lower-energy region can be attributed to a mixture of spin-allowed singlet metal-to-ligand charge transfer (¹MLCT) and spin-forbidden ³MLCT transitions [17].

Complex **1** emits orange–red light in toluene solution with an emission maximum at 592 nm, while **3** in toluene

solution exhibits a featureless emission peak at 551 nm, which falls in the yellowish green region. The color tuning of the two complexes results from the influence on the electronic properties of the appended charge-transporting moieties on the complexes [18]. The geometry were optimized at B3LYP/6-31G(d) level, and the electronic properties of the compounds were calculated at tHCTHhyb/6-311++G(d, p) level (for details, see Section 4). As shown in Fig. S2, the HOMOs consist of a mixture of π -orbitals of phenyl ring in 2-phenylpyridine (ppy) ligand and *d*-orbitals of Ir, whereas the LUMOs delocalize on the ligand with predominant contribution from the pyridyl π -orbitals, which coincide with the literature results [19]. For compound **1** and **2**, the HOMO orbitals extend to the electron-donating diphenylamine/carbazole groups on the phenyl ring. In general, the introduction of electron-donating or -withdrawing groups will increase or decrease the HOMO level, respectively; while the electron-acceptors will stabilize the LUMO more than the electron-donors. In addition, the extended conjugation of the ligand will narrow the band gap to some extent. The above-mentioned three factors contribute to color-tuning of the phosphors. For example, complex **3** emits yellowish green light due to the decreased HOMO energy level by phosphine oxide,

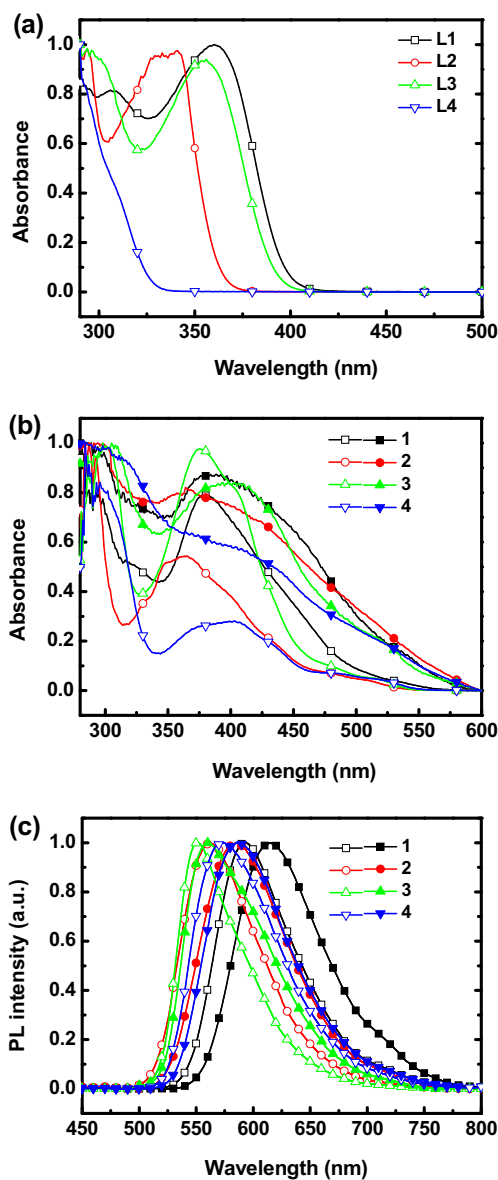


Fig. 2. (a) UV-vis absorption spectra of the ligands in toluene solution, (b) UV-vis absorption spectra and (c) PL spectra of the phosphors **1–4** recorded both in toluene (open) and films (solid).

Table 1

Photophysical, electrochemical and thermal data of **1–4**.

	1	2	3	4
T_g/T_d (°C)	247/499	268/505	246/486	284/500
λ_{abs} (nm) ^a	288/375	287/364	293/377	291/401
λ_{abs} (nm) ^b	295/379	293/365	305/404	312/418
$\lambda_{\text{em,max}}$ (nm) ^a	592	562	551	572
$\lambda_{\text{em,max}}$ (nm) ^b	615	585	560	586
Φ (%) ^c	43 (21)	46 (33)	55 (29)	51 (24)
HOMO/LUMO (eV) ^d	−4.92/−2.56	−5.20/−2.60	−5.35/−2.40	−5.33/−2.51

^a Measured in toluene with a concentration of 10^{-5} M.

^b Neat film data (measured with the excitation wavelength of 420 nm for the PL spectra).

^c Solid state quantum yields using an integration sphere were measured at 298 K in PMMA at 10 wt.%, values in neat films are in parenthesis. All PLQYs are $\pm 5\%$.

^d The HOMO energies were estimated from the half-wave potentials and the LUMO energies were deduced from the energy gap (E_g) and HOMO.

the increased LUMO energy level by triphenylamine unit and the increased conjugation.

Solid state photoluminescence quantum yields (PLQYs) of the complexes were measured using an integrating sphere apparatus on the quartz plate and the data are listed in Table 1. The PLQYs of the four complexes after doped into poly(methyl methacrylate) (PMMA) matrix at 10% by weight are in the range of 43–55% [20]; it is noteworthy that the PLQYs in neat films is not significantly dropped, remaining in the range of 21–33%. This indicates that the iridium complexes appended with bulky electron-acceptor arylphosphine oxide and different electron-donors provide good encapsulation for emissive core and effectively suppress the intermolecular interactions [21].

2.4. Electrochemical properties

Cyclic voltammetry (CV) was performed to investigate the electrochemical behaviors of **1–4** (Fig. 3). The HOMO energy levels of the compounds were determined from the half-wave potentials with regard to the energy level of ferrocene (−4.8 eV below vacuum); no reduction data was observed, and thus the LUMO levels were deduced from HOMO energy levels and optical band gaps determined by the onset of absorption. As mentioned above, the strong donor will destabilize the metal d-orbital, leading to the high HOMO energy level. Complex **1** with the strongest electron-donating group has the highest HOMO energy level, which is close to the work function of common anode buffer layer PEDOT:PSS (−4.80 eV) and thus beneficial for the facile charge injection into emission layer (EML). The HOMO level decreased in the following order: **1** > **2** > **3** \approx **4** (Table 1), which coincides well with the order of the electron-donating abilities of the substitutes on the ligand.

2.5. Electrophosphorescence

To evaluate the phosphors as self-host phosphorescent emitters, nondoped PhOLEDs were fabricated with typical double-layer configuration as follows: ITO/poly(ethylene-dioxythiophene):poly(styrenesulfonate) (PEDOT:PSS, 50 nm)/iridium complexes (80 nm)/1,3,5-tris(*N*-phenylbenzimidazol-2-yl)benzene (TPBI, 25 nm)/CsF (1.5 nm)/Al (150 nm). In this sandwich geometry, TPBI and CsF act

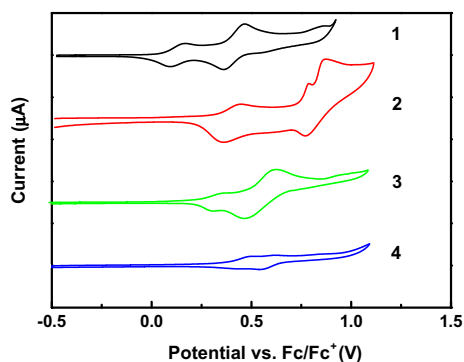


Fig. 3. Oxidation scan curves of cyclic voltammograms for the complexes in CH_2Cl_2 .

as electron-transporting layer (ETL) and electron-injecting layer (EIL), respectively. Fig. 4 shows the EL spectra, current density–voltage–brightness (J – V – L) characteristics, and efficiency versus current density curves of the devices, and Table 2 summarizes the EL data. The electroluminescence (EL) devices display identical spectra with their PL counterparts without additional emission from the aggregation or the ligands. This further proves that these first-generation functional iridium dendrimers could be used alone as EML. The driving voltage decreased in the following order: $1 > 2 > 3 \approx 4$, which coincides well with the sequence of the HOMO levels. The low turn-on voltage for **1** (3.5 V) can be attributed to the small energy barrier between PEDOT:PSS and EML. Low-lying HOMO levels caused by the electron-withdrawing phosphine oxide group in **3** and **4** partially induced large turn-on voltages of the devices due to the retarded hole-injection from anode buffer layer to EML. Meanwhile, we note that the devices for **2–4** exhibit relative low leakage current in the small voltage region (0–4 V). For instance, the leakage current before turn-on for the device based on **2** is around $10^{-3} \text{ mA cm}^{-2}$, which suggests good surface morphology of the EML. However, the leakage current for the device based on **1** is as high as $10^{-1} \text{ mA cm}^{-2}$, which may leads to the fair device performance.

Device with complex **1** as EML exhibits the lowest current efficiency of 2.4 cd A^{-1} with red light emission. For the complex **2**, the device achieves the maximum current efficiency of 12.4 cd A^{-1} and maximum external quantum efficiency of 8.8% at a luminance of 250 cd m^{-2} , which are comparable to the best performances of the solution-processed orange–red emitting PhOLEDs [22]. Even at a practical luminance of 1000 cd m^{-2} , the values are maintained as high as 11.5 cd A^{-1} and 8.2%. The small efficiency roll-off values should be attributed to the sufficiently depressed concentration quenching of emissive core and the bipolar charge-transporting abilities of the ligands containing electron-donating carbazole and electron-accepting phosphine oxide unit. The devices based on complexes **3** and **4** show fair efficiencies in comparison with the device based on complex **2**. To get insight into the origin of lower EL efficiencies in the devices based on complexes **3** and **4**, charge transporting properties of the complexes were

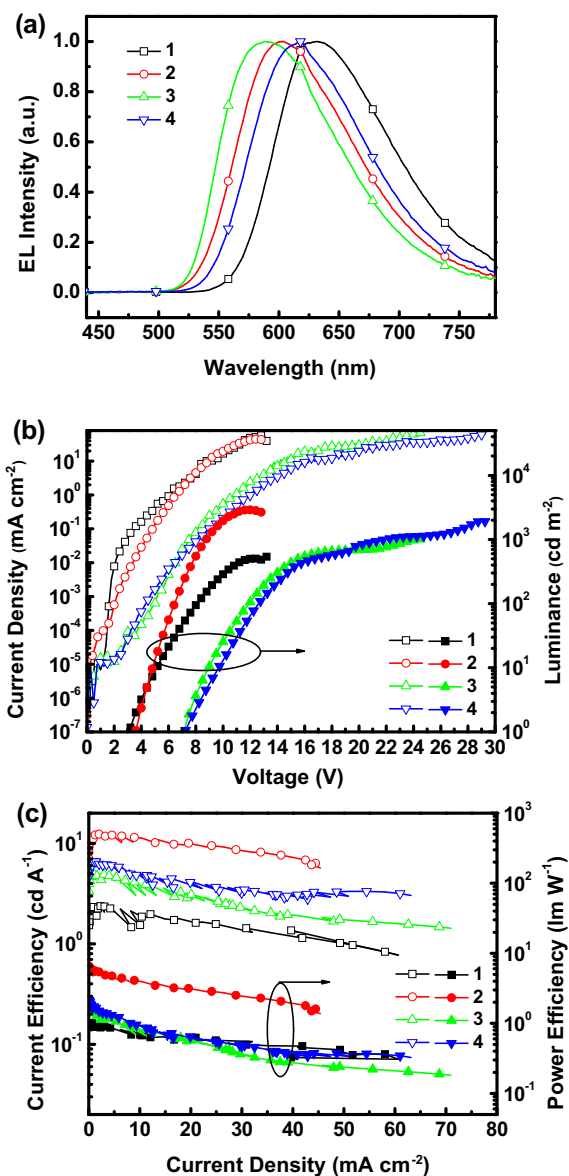


Fig. 4. (a) EL spectra at applied voltage of 10 V; (b) current density–voltage–luminance characteristics; (c) current efficiency and power efficiency versus current density curves for devices.

investigated. We measure J – V characteristics of the electron-only devices and hole-only devices, with device structures of ITO/Al (40 nm)/emitting layer (100 nm)/CsF (1.5 nm)/Al (100 nm) and ITO/PEDOT4083 (40 nm)/emitting layer (100 nm)/ MoO_3 (10 nm)/Al (100 nm), respectively. The deduced electron mobilities using the space-charge-limited-current (SCLC) model from the J – V characteristics of single charge carrier devices for **1–4** are 1.6×10^{-5} , 1.0×10^{-5} , 7.8×10^{-6} , and $1.8 \times 10^{-5} \text{ cm}^2 \text{ V}^{-1} \text{ s}^{-1}$, respectively; while the hole mobilities are 1.5×10^{-7} , 1.5×10^{-8} , 1.1×10^{-8} , and $3.7 \times 10^{-9} \text{ cm}^2 \text{ V}^{-1} \text{ s}^{-1}$, respectively. On the basis of these observations, we concluded that relatively lower efficiencies in the devices based on complexes **3** and **4** can be partially

Table 2

Electroluminescence data of the devices.

EML	V _{on} ^a (V)	L _{max} ^b /V (cd m ⁻²)	η _c ^c (cd A ⁻¹)	η _p ^d (lm W ⁻¹)	η _{EQE} ^e (%)	CIE ^f (x, y)
1	3.5	541/13.4	2.4	1.0	3.0	0.64, 0.35
2	3.7	2900/12.0	12.4	6.6	8.8	0.57, 0.42
3	7.0	1016/24.8	5.2	1.8	3.1	0.54, 0.45
4	7.0	1937/29.0	6.6	2.2	5.4	0.59, 0.40

^a Turn-on voltage.^b Maximum luminance.^c Maximum current efficiency.^d Maximum power efficiency.^e Maximum external quantum efficiency.^f Measured at 10 V.

attributed to the more severe carrier imbalance due to the electron-withdrawing substitutes on the phenyl ring, which has little contribution to hole injection to the EML and hole transportation therein. On the other side, it is not clear at this stage why complexes **1** showed inferior devices than complexes **2** even the former exhibited better charge transporting properties.

3. Conclusions

In summary, we have designed and synthesized a series of new homoleptic Ir(III) complexes by integrating with different charge-transporting moieties onto the emissive core to achieve charge balance in the EML while maintain the self-host ability of the phosphors. For the device using **2** as neat emitter, a maximum external efficiency of 8.8% is realized with small value (6.8%) of efficiency roll-off at high brightness. This indicates that rational incorporation of charge-transporting moieties into the sphere of iridium(III) core is a simple and effective approach to develop efficient host-free phosphors for solution-processable nondoped PhOLEDs. We believe that this strategy of bipolar phosphors would be applicable to generate novel phosphorescent materials that have emission colors covering the whole visible region for use in multicolor OLEDs.

4. Experimental

4.1. General information

¹H NMR and ¹³C NMR spectra were measured on a MECUYR-VX300 spectrometer. Elemental analyses of carbon, hydrogen, and nitrogen were performed on a Vario EL III microanalyzer. Melting points of the solids were measured on X-4 melting point apparatus and uncorrected. Mass spectra were measured on a ZAB 3F-HF mass spectrophotometer or Bruker BIFLEX III TOF mass spectrometer. UV-vis absorption spectra were conducted on a Shimadzu UV-2500 recording spectrophotometer. Photoluminescent (PL) spectra were recorded on a Hitachi F-4500 fluorescence spectrophotometer. The solid state PL quantum efficiencies (PLQYs) were measured using an integration sphere. Differential scanning calorimetry (DSC) was performed on a NETZSCH DSC 200 PC unit at a heating rate of 10 °C min⁻¹ from room temperature to 400 °C under a flow of nitrogen. Thermogravimetric analysis (TGA) was undertaken with a NETZSCH STA 449C instrument. The

thermal stability of the samples under a nitrogen atmosphere was determined by measuring their weight loss while heating at a rate of 15 °C min⁻¹ from 25 to 800 °C. Cyclic voltammetry (CV) was carried out in nitrogen-purged dichloromethane (oxidation scan) at room temperature with a CHI voltammetric analyzer. Tetrabutylammonium hexafluorophosphate (TBAPF6) (0.1 M) was used as the supporting electrolyte. The conventional three-electrode configuration consists of a platinum working electrode, a platinum wire auxiliary electrode, and an Ag wire pseudo-reference electrode with ferrocenium-ferrocene (Fc⁺/Fc) as the internal standard. Cyclic voltammograms were obtained at scan rate of 100 mV s⁻¹. The onset potential was determined from the intersection of two tangents drawn at the rising and background current of the cyclic voltammogram.

4.2. Computational details

The geometrical and electronic properties were performed with the Gaussian 09 program package. The calculation was optimized by means of the B3LYP (Becke three parameters hybrid functional with Lee–Yang–Perdew correlation functionals) with the 6-31G(d) atomic basis set.³² Then the electronic structures were calculated at rHCTHhyb/6-311++G(d, p) level. Molecular orbitals were visualized using Gaussview.

4.3. Device fabrication and measurement

Patterned indium tin oxide (ITO)-coated glass substrates with a sheet resistance of 15–20 Ω/square underwent a wet-cleaning course in an ultrasonic bath, beginning with acetone, followed by detergent, deionized water, and isopropanol. After oxygen-plasma treatment, a 50 nm thick anode buffer layer of PEDOT:PSS (Baytron P 4083, Bayer AG) film was spin-cast on the ITO substrate and dried by baking in vacuum oven at 80 °C overnight. The emitting layer was prepared by spin-coating from chlorobenzene solution of the dendrimers on top of the PEDOT layer, then annealed at 100 °C for 20 min. TPBI (25 nm), Ba (4 nm) and Al (150 nm) were evaporated with a shadow mask successively at a base pressure of 3 × 10⁻⁴ Pa. The thickness of the evaporated TPBI and cathode was monitored by a quartz-crystal thickness/ratio monitor (Sycon model STM-100/MF). The cross-sectional area between the cathode and anode defined the pixel size

of 19 mm². Except for the spin coating of the PEDOT layer, all the processes were carried out in the controlled atmosphere of a nitrogen dry-box (Vacuum Atmosphere Co.) containing less than 1 ppm oxygen and moisture. All measurements were carried out at room temperature under ambient conditions.

4.4. Synthesis of materials

Starting chemicals and reagents were purchased from commercial sources and used as received without further purification. Solvents for synthesis were purified according to standard procedures prior to use. All reactions were performed under an inner argon atmosphere. Synthesis of 4-(diphenylamino)phenylboronic acid, 9-(4-(4,4,5,5-tetramethyl-1,3,2-dioxaborolan-2-yl)phenyl)-9H-carbazole and 4-bromophenyldiphenylphosphine oxide were proceeded following the reported procedures [23–25].

4.4.1. 4-(4-Bromopyridin-2-yl)-N,N-diphenylaniline (**5**)

Degassed THF (81 mL) was added to a mixture of 4-(diphenylamino)phenylboronic acid (5.23 g, 18.00 mmol), 2,4-dibromopyridine (5.12 g, 21.60 mmol), Na₂CO₃ (2 M, 27 mL, 54.00 mmol) and Pd(PPh₃)₄ (0.21 g, 0.18 mmol). The mixture was refluxed for 24 h under argon. After cooling to room temperature, the solvent was evaporated under reduced pressure. The residue was poured into water (40 mL) and then extracted with CH₂Cl₂ (100 mL *3). The organic extracts were collected and dried with anhydrous Na₂SO₄. After filtered and removal of the solvent, the residue was purified by column chromatography on silica gel (eluent: petroleum/ethyl acetate = 5:1, v/v) to give **5** as white solid (5.06 g, 70%). mp: 108–110 °C. ¹H NMR (300 MHz, CDCl₃): δ 8.45 (d, *J* = 4.5 Hz, 1H), 7.85 (s, 1H), 7.82 (d, *J* = 7.2 Hz, 2H), 7.34 (d, *J* = 4.5 Hz, 1H), 7.28 (d, *J* = 6.9 Hz, 4H), 7.14–7.09 (m, 6H), 7.06 (d, *J* = 7.2 Hz, 2H); ¹³C NMR (75 MHz, CDCl₃): δ 158.18, 149.99, 149.08, 147.05, 133.19, 131.04, 129.20, 127.68, 124.76, 124.27, 123.34, 122.81, 122.49; MS (EI): *m/z* 401 [M]⁺. Anal. Calcd. for C₂₃H₁₇BrN₂: C 68.84, H 4.27, N 6.98; found: C 69.01, H 4.15, N 6.67.

4.4.2. (4-(4,4,5,5-Tetramethyl-1,3,2-dioxaborolan-2-yl)phenyl)diphenyl phosphine oxide (**6**)

4-Bromophenyldiphenylphosphine oxide (6.18 g, 17.30 mmol), bis(pinacolato)diborane (4.83 g, 19.03 mmol), and KOAc (5.94 g, 60.55 mmol) were mixed together in a 150 mL flask. After degassing, dry dioxane (80 mL) was added to the mixture under flow of argon. Afterward, [Pd(dppf)Cl₂] (150 mg, dppf = 1,1'-bis(diphenylphosphanyl)ferrocene) was added. The reaction mixture was kept at 85 °C overnight and then cooled to room temperature. The solvent was concentrated and the inorganic salt was dissolved completely after addition of water (50 mL). After extracted with CH₂Cl₂ (100 mL *3), the combined organic layer was washed with brine (30 mL) and then dried over anhydrous Na₂SO₄. The crude product was purified by silica gel column chromatography (eluent: CH₂Cl₂/methanol = 30:1, v/v) to yield the desired compound as colorless oil (6.43 g, 92%). ¹H NMR (300 MHz, CDCl₃): δ 7.89 (d, *J* = 7.2 Hz, 2H), 7.66 (d, *J* = 7.8 Hz, 4H), 7.52 (d, *J* = 7.2 Hz,

2H), 7.48–7.45 (m, 6H), 1.33 (s, 12H); ¹³C NMR (75 MHz, CDCl₃): δ 134.85, 134.69, 132.30, 132.19, 131.44, 131.32, 128.80, 128.64, 82.27, 24.79; MS (EI): *m/z* 403 [M]⁺. Anal. Calcd. for C₂₄H₂₆BO₃P: C 71.31, H 6.48; found: C 71.62, H 6.76.

L1: degassed toluene (45 mL) and ethanol (15 mL) were added to a mixture of **5** (3.11 g, 7.76 mmol), **6** (3.76 g, 9.30 mmol), Na₂CO₃ (2 M, 15 mL, 30.00 mmol) and Pd(PPh₃)₄ (0.18 g, 0.16 mmol). The resulting mixture was stirred and heated to reflux for 48 h under argon atmosphere. After cooling to room temperature, the solvent was evaporated under reduced pressure and taken up with CH₂Cl₂ (120 mL). The organic layer was washed with brine (30 mL) and water (30 mL) sequentially and dried over anhydrous Na₂SO₄. After filtered, the solvent was evaporated to dryness and subjected to column chromatography on silica gel (eluent: CH₂Cl₂/methanol = 30:1, v/v) to give **L1** as yellow solid (2.32 g, 50%). mp: 104–110 °C. ¹H NMR (300 MHz, CDCl₃): δ 8.71 (d, *J* = 5.4 Hz, 1H), 7.91 (s, 1H), 7.89 (d, *J* = 5.1 Hz, 1H), 7.85 (d, *J* = 7.5 Hz, 2H), 7.78 (d, *J* = 7.8 Hz, 2H), 7.71–7.67 (m, 4H), 7.58 (d, *J* = 7.2 Hz, 2H), 7.51–7.49 (m, 4H), 7.30–7.28 (m, 6H), 7.15–7.08 (m, 6H), 7.08–7.03 (m, 2H); ¹³C NMR (75 MHz, CDCl₃): δ 157.37, 149.73, 148.53, 146.91, 141.71, 132.50, 132.38, 131.69, 131.57, 130.95, 128.95, 128.37, 128.18, 127.51, 126.90, 126.74, 124.37, 122.98, 122.54, 119.18, 117.62; MS (EI): *m/z* 598 [M]⁺; Anal. Calcd. for C₄₁H₃₁N₂O: C 82.26, H 5.22, N 4.68; found: C 82.03, H 4.93, N 4.57.

4.4.3. 9-(4-(4-Bromopyridin-2-yl)phenyl)-9H-carbazole (**7**)

According to the similar procedure for the preparation of **5**, degassed THF (100 mL) was added to a mixture of 9-(4-(4,4,5,5-tetramethyl-1,3,2-dioxaborolan-2-yl)phenyl)-9H-carbazole (8.20 g, 22.15 mmol) and 2,4-dibromopyridine (5.25 g, 22.15 mmol), Na₂CO₃ (2 M, 33 mL, 66.00 mmol) and Pd(PPh₃)₄ (0.25 g, 0.22 mmol). The mixture was refluxed for 24 h under argon. After cooling to room temperature, the solvent was evaporated under reduced pressure. The residue was poured into water (40 mL) and then extracted with CH₂Cl₂ (100 mL *3). The organic extracts were collected and dried with anhydrous Na₂SO₄. After filtered and removal of the solvent, the residue was purified by column chromatography on silica gel (eluent: petroleum/ethyl acetate = 5:1, v/v) to give **7** as white solid (5.65 g, 64%). mp: 137–139 °C. ¹H NMR (300 MHz, CDCl₃): δ 8.57 (d, *J* = 5.4 Hz, 1H), 8.22 (d, *J* = 8.1 Hz, 2H), 8.17 (d, *J* = 7.8 Hz, 2H), 7.99 (s, 1H), 7.71 (d, *J* = 8.4 Hz, 2H), 7.49 (d, *J* = 5.7 Hz, 1H), 7.45–7.40 (m, 4H), 7.33 (d, *J* = 7.2 Hz, 2H); ¹³C NMR (75 MHz, CDCl₃): δ 157.40, 150.10, 140.23, 138.65, 136.35, 133.33, 128.18, 126.71, 125.81, 125.15, 123.42, 123.31, 120.12, 119.98, 109.52; MS (EI): *m/z* 400 [M]⁺. Anal. Calcd. for C₂₃H₁₅BrN₂: C 69.19, H 3.79, N 7.02; found: C 69.28, H 3.66, N 7.17.

L2: according to the similar procedure for the preparation of **L1**, degassed toluene (30 mL) and ethanol (10 mL) were added to a mixture of **7** (2.00 g, 5.00 mmol), **6** (2.83 g, 7.00 mmol), Na₂CO₃ (2 M, 10 mL, 20.00 mmol) and Pd(PPh₃)₄ (0.11 g, 0.10 mmol). The resulting mixture was stirred and heated to reflux for 48 h under argon atmosphere. After cooling to room temperature, the solvent was evaporated under reduced pressure and taken

up with CH_2Cl_2 (120 mL). The organic layer was washed with brine (30 mL) and water (30 mL) sequentially and dried over anhydrous Na_2SO_4 . After filtered, the solvent was evaporated to dryness and subjected to column chromatography on silica gel (eluent: CH_2Cl_2 /methanol = 30:1, v/v) to give **L2** as yellow solid (2.63 g, 88%). mp: 275–277 °C. ^1H NMR (300 MHz, CDCl_3): δ 8.82 (d, J = 5.7 Hz, 1H), 8.34 (s, 1H), 8.27 (d, J = 7.2 Hz, 2H), 8.19 (d, J = 5.1 Hz, 1H), 8.15 (d, J = 8.2 Hz, 2H), 8.02 (d, J = 7.5 Hz, 2H), 7.88–7.83 (m, 4H), 7.73–7.70 (m, 6H), 7.65–7.50 (m, 8H), 7.31–7.28 (m, 2H); ^{13}C NMR (75 MHz, CDCl_3): δ 156.74, 149.95, 147.76, 141.37, 140.13, 138.09, 137.51, 132.54, 131.80, 131.55, 130.91, 128.33, 126.92, 126.76, 126.62, 125.64, 123.06, 120.08, 119.89, 119.76, 118.29, 109.38; MS (EI): m/z 596 $[M]^+$; Anal. Calcd. for $\text{C}_{41}\text{H}_{29}\text{N}_2\text{OP}$: C 82.53, H 4.90, N 4.70; found: C 82.30, H 5.12, 4.57.

4.4.4. 4-Bromo-2-(4-(diphenylphosphoryl)phenyl)pyridine (**8**)

According to the similar procedure for the preparation of **5**, degassed THF (45 mL) was added to a mixture of **6** (4.04 g, 10.00 mmol), 2,4-dibromopyridine (2.84 g, 12.00 mmol), Na_2CO_3 (2 M, 15 mL, 30.00 mmol) and $\text{Pd}(\text{PPh}_3)_4$ (0.12 g, 0.10 mmol). The mixture was refluxed for 24 h under argon. After cooling to room temperature, the solvent was evaporated under reduced pressure. The residue was poured into water (40 mL) and then extracted with CH_2Cl_2 (100 mL *3). The organic extracts were collected and dried with anhydrous Na_2SO_4 . After filtered and removal of the solvent, the residue was purified by column chromatography on silica gel (eluent: CH_2Cl_2 /methanol = 30:1, v/v) to give **8** as white solid (2.34 g, 54%). mp: 134–136 °C. ^1H NMR (300 MHz, CDCl_3): δ 8.53 (d, J = 5.1 Hz, 1H), 8.45 (d, J = 5.1 Hz, 1H), 8.07 (d, J = 7.2 Hz, 2H), 7.93 (s, 1H), 7.83 (d, J = 7.8 Hz, 2H), 7.72 (d, J = 6.6 Hz, 4H), 7.57–7.53 (m, 6H); ^{13}C NMR (75 MHz, CDCl_3): δ 157.70, 151.00, 141.62, 134.05, 132.90, 129.07, 128.02, 127.32, 126.30, 124.66, 121.32; MS (EI): m/z 434 $[M]^+$. Anal. Calcd. for $\text{C}_{23}\text{H}_{17}\text{BrNOP}$: C 63.61, H 3.95, N 3.23; found: C 63.87, H 4.12, N 3.09.

L3: according to the similar procedure for the preparation of **L1**, degassed toluene (30 mL) and ethanol (10 mL) were added to a mixture of **8** (2.44 g, 5.60 mmol) and 4-(diphenylamino)phenylboronic acid (2.44 g, 8.40 mmol), Na_2CO_3 (2 M, 10 mL, 20.00 mmol) and $\text{Pd}(\text{PPh}_3)_4$ (0.13 g, 0.11 mmol). The resulting mixture was stirred and heated to reflux for 48 h under argon atmosphere. After cooling to room temperature, the solvent was evaporated under reduced pressure and taken up with CH_2Cl_2 (120 mL). The organic layer was washed with brine (30 mL) and water (30 mL) sequentially and dried over anhydrous Na_2SO_4 . After filtered, the solvent was evaporated to dryness and subjected to column chromatography on silica gel (eluent: CH_2Cl_2 /methanol = 30:1, v/v) to give **L3** as yellow solid (1.11 g, 33%). mp: 107–114 °C. ^1H NMR (300 MHz, CDCl_3): δ 8.82 (d, J = 5.4 Hz, 1H), 8.30 (d, J = 7.2 Hz, 2H), 8.17 (d, J = 7.5 Hz, 2H), 8.03 (s, 1H), 7.88–7.83 (m, 5H), 7.72 (d, J = 6.9 Hz, 6H), 7.57–7.43 (m, 12H), 7.33–7.31 (m, 2H); ^{13}C NMR (75 MHz, CDCl_3): δ 156.13, 149.73, 148.55, 146.63, 142.46, 132.59, 132.13, 131.58, 130.28, 128.97, 128.16, 128.00, 127.27, 126.69, 126.53,

124.50, 123.21, 122.32, 119.74, 117.89; MS (EI): m/z 598 $[M]^+$; Anal. Calcd. for $\text{C}_{41}\text{H}_{31}\text{N}_2\text{OP}$: C 82.26, H 5.22, N 4.68; found: C 82.30, H 4.89, 4.54.

L4: according to the similar procedure for the preparation of **L1**, degassed toluene (72 mL) and ethanol (24 mL) were added to a mixture of 2,4-dibromopyridine (1.90 g, 8.00 mmol) and **6** (8.08 g, 20.00 mmol), Na_2CO_3 (2 M, 24 mL, 48.00 mmol) and $\text{Pd}(\text{PPh}_3)_4$ (0.37 g, 0.32 mmol). The resulting mixture was stirred and heated to reflux for 48 h under argon atmosphere. After cooling to room temperature, the solvent was evaporated under reduced pressure and taken up with CH_2Cl_2 (120 mL). The organic layer was washed with brine (30 mL) and water (30 mL) sequentially and dried over anhydrous Na_2SO_4 . After filtered, the solvent was evaporated to dryness and subjected to column chromatography on silica gel (eluent: CH_2Cl_2 /methanol = 20:1, v/v) to give **L4** as yellow solid (2.70 g, 53%). mp: 246–247 °C. ^1H NMR (300 MHz, CDCl_3): δ 8.79 (d, J = 5.4 Hz, 1H), 8.12 (d, J = 7.5 Hz, 2H), 7.95 (s, 1H), 7.84–7.79 (m, 5H), 7.70–7.67 (m, 8H), 7.56–7.50 (m, 14H); ^{13}C NMR (75 MHz, CDCl_3): δ 156.21, 149.89, 147.61, 141.90, 140.90, 133.53, 133.10, 132.35, 132.01, 131.89, 131.32, 130.97, 128.07, 126.60, 126.45, 120.47, 118.60; MS (EI): m/z 630 $[M]^+$; Anal. Calcd. for $\text{C}_{41}\text{H}_{31}\text{NO}_2\text{P}_2$: C 77.96, H 4.95, N 2.22; found: C 77.76, H 4.89, 2.08.

4.4.5. Preparation of the homoleptic complex **1**

L1 (1.02 g, 1.70 mmol) and $\text{Ir}(\text{acac})_3$ (0.25 g, 0.50 mmol) were added to a 50 mL round-necked flask. Thereafter, distilled *o*-dichlorobenzene (5 mL), 2-(2-methoxyethoxy)ethanol (10 mL) and glycerol (15 mL) were to the flask sequentially. The mixture was heated to 230 °C for 36 h. After completion, *o*-dichlorobenzene was removed under reduced pressure. The mixture was poured into H_2O and extracted with CH_2Cl_2 . The organic phase was washed with brine and dried over anhydrous Na_2SO_4 . The solvent was evaporated under reduced pressure and the residue was purified through column chromatography with CH_2Cl_2 /methanol (20:1, v/v) as eluent to afford **1** (0.95 g) as red powder with a yield of 95%. ^1H NMR (300 MHz, CDCl_3): δ 7.88 (s, 3H), 7.74–7.71 (m, 18H), 7.55–7.49 (m, 15H), 7.36 (d, J = 7.8 Hz, 6H), 7.12–7.09 (m, 12H), 6.85–6.82 (m, 18H), 6.68–6.63 (m, 12H), 6.27–6.20 (m, 6H); ^{13}C NMR (75 MHz, CDCl_3): δ 166.97, 162.22, 148.82, 147.87, 147.69, 146.84, 142.00, 137.21, 133.12, 132.68, 132.42, 132.27, 131.16, 130.12, 128.85, 127.33, 127.26, 125.14, 124.98, 122.66, 119.18, 115.76, 114.89; MALDI-TOF: Calcd. for $\text{C}_{123}\text{H}_{90}\text{IrN}_6\text{O}_3\text{P}_3$ 1985.2; found 1985.2; Anal. Calcd. for $\text{C}_{123}\text{H}_{90}\text{IrN}_6\text{O}_3\text{P}_3$: C 74.42, H 4.57, N 4.23; found: C 74.50, H 4.63, N 4.02.

4.4.6. Preparation of the homoleptic complex **2**

90% ^1H NMR (300 MHz, CDCl_3): δ 8.17 (s, 3H), 7.94 (d, J = 6.9 Hz, 6H), 7.87 (s, 3H), 7.82–7.79 (m, 12H), 7.72–7.66 (m, 18H), 7.57 (d, J = 6.3 Hz, 6H), 7.50–7.48 (m, 12H), 7.07–7.01 (m, 18H), 6.85–6.82 (m, 6H); ^{13}C NMR (75 MHz, CDCl_3): δ 165.22, 159.36, 149.76, 148.42, 148.11, 147.54, 147.22, 134.36, 132.02, 131.89, 131.79, 131.34, 129.78, 128.67, 128.52, 128.28, 128.12, 127.97, 125.50, 124.21, 122.64, 120.58, 116.68; MALDI-TOF: Calcd. for $\text{C}_{123}\text{H}_{84}\text{IrN}_6\text{O}_3\text{P}_3$ 1979.2; found 1979.1; Anal. Calcd. for

$C_{123}H_{84}IrN_6O_3P_3$: C 74.64, H 4.28, N 4.25; found: C 74.27, H 4.25, N 4.02.

4.4.7. Preparation of the homoleptic complex 3

90% 1H NMR (300 MHz, $CDCl_3$): δ 7.95 (s, 3H), 7.67 (d, $J = 5.4$ Hz, 3H), 7.55 (d, $J = 7.8$ Hz, 12H), 7.39 (s, 3H), 7.35–7.28 (m, 24H), 7.18 (d, $J = 7.8$ Hz, 24H), 7.12 (d, $J = 6.6$ Hz, 12H), 7.02–7.00 (m, 6H), 6.65–6.60 (m, 3H); ^{13}C NMR (75 MHz, $CDCl_3$): δ 167.49, 163.11, 149.11, 148.77, 143.01, 142.17, 141.27, 140.16, 134.71, 134.04, 133.36, 133.13, 132.50, 129.90, 128.35, 126.66, 124.33, 120.82, 119.42, 118.13, 111.53; MALDI-TOF: Calcd. for $C_{123}H_{90}IrN_6O_3P_3$ 1985.2; found 1985.4; Anal. Calcd. for $C_{123}H_{90}IrN_6O_3P_3$: C 74.42, H 4.57, N 4.23; found: C 74.66, H 4.56, N 4.05.

4.4.8. Preparation of the homoleptic complex 4

82% 1H NMR (300 MHz, $CDCl_3$): δ 7.97 (s, 3H), 7.84 (d, $J = 8.4$ Hz, 6H), 7.75–7.72 (m, 18H), 7.58–7.50 (m, 18H), 7.36–7.28 (m, 18H), 7.21–7.16 (m, 18H), 7.01–6.98 (m, 6H), 6.65–6.61 (m, 3H); ^{13}C NMR (75 MHz, $CDCl_3$): δ 165.70, 158.92, 148.11, 147.00, 140.89, 139.58, 134.80, 133.33, 132.51, 132.30, 131.98, 131.76, 128.97, 128.65, 128.28, 127.43, 124.49, 121.76, 117.78; MALDI-TOF: Calcd. for $C_{123}H_{90}IrN_3O_6P_6$ 2084.1; found 2084.2; Anal. Calcd. for $C_{123}H_{90}IrN_3O_6P_6$: C 70.88, H 4.35, N 2.02; found: C 70.63, H 4.73, N 1.81.

Author contributions

The manuscript was written through contributions of all authors. All authors have given approval to the final version of the manuscript.

Acknowledgements

C. Yang thanks the National Basic Research Program of China (973 Program 2013CB834805), and the National Science Fund for Distinguished Young Scholars of China (No. 51125013). H. Wu thanks the National Natural Science Foundation of China (61177022).

Appendix A. Supplementary material

Supplementary data associated with this article can be found, in the online version, at <http://dx.doi.org/10.1016/j.orgel.2014.04.008>.

References

- [1] (a) M.A. Baldo, D.F. O'Brien, Y. You, A. Shoustikov, S. Sibley, M.E. Thompson, S.R. Forrest, *Nature* 395 (1998) 151; (b) X. Gong, W. Ma, J.C. Ostrowski, G.C. Bazan, A.J. Heeger, *Adv. Mater.* 16 (2004) 615.
- [2] (a) M.A. Baldo, S. Lamansky, P.E. Burrows, M.E. Thompson, S.R. Forrest, *Appl. Phys. Lett.* 75 (1999) 4; (b) L. Xiao, Z. Chen, B. Qu, J. Luo, S. Kong, Q. Gong, J. Kido, *Adv. Mater.* 23 (2011) 926; (c) Y. Chi, P.-T. Chou, *Chem. Soc. Rev.* 39 (2010) 638.
- [3] (a) C. Ulbricht, B. Beyer, C. Friebe, A. Winter, U.S. Schubert, *Adv. Mater.* 21 (2009) 4418; (b) Y. Liu, K. Ye, Y. Fan, W. Song, Y. Wang, Z. Hou, *Chem. Commun.* (2009) 3699.
- [4] (a) R. Wang, D. Liu, H. Ren, T. Zhang, H. Yin, G. Liu, J. Li, *Adv. Mater.* 23 (2011) 2823; (b) H. Wu, G. Zhou, J. Zou, C.-L. Ho, W.-Y. Wong, W. Yang, J. Peng, Y. Cao, *Adv. Mater.* 21 (2009) 4181; (c) C.-H. Chang, Y.-H. Lin, C.-C. Chen, C.-K. Chang, C.-C. Wu, L.-S. Chen, W.-W. Wu, Y. Chi, *Org. Electron.* 10 (2009) 1235.
- [5] Q. Wang, D. Ma, *Chem. Soc. Rev.* 39 (2010) 2387.
- [6] (a) F. So, B. Krummacker, M.K. Mathai, D. Poplavskyy, S.A. Choulis, V.-E. Choong, *J. Appl. Phys.* 102 (2007) 091101; (b) C. Zhong, C. Duan, F. Huang, H. Wu, Y. Cao, *Chem. Mater.* 23 (2011) 326; (c) H. Wu, L. Ying, W. Yang, Y. Cao, *Chem. Soc. Rev.* 38 (2009) 3391.
- [7] (a) Y. Tao, C. Yang, J. Qin, *Chem. Soc. Rev.* 40 (2011) 2943; (b) S. Gong, C. Yang, J. Qin, *Chem. Soc. Rev.* 41 (2012) 4797.
- [8] (a) C. Yang, X. Zhang, H. You, L. Zhu, L. Chen, L. Zhu, Y. Tao, D. Ma, Z. Shuai, J. Qin, *Adv. Funct. Mater.* 17 (2007) 651; (b) L. Chen, H. You, C. Yang, X. Zhang, J. Qin, D. Ma, *J. Mater. Chem.* 16 (2006) 3332; (c) L. Chen, C. Yang, J. Qin, J. Gao, D. Ma, *Inorg. Chim. Acta* 359 (2006) 4207; (d) X. Zhang, J. Gao, C. Yang, L. Zhu, Z. Li, K. Zhang, J. Qin, H. You, D. Ma, *J. Organomet. Chem.* 691 (2006) 4312; (e) L. Chen, C. Yang, M. Li, J. Qin, J. Gao, H. You, D. Ma, *Cryst. Growth Des.* 7 (2007) 39; (f) L. Chen, C. Yang, J. Qin, J. Gao, H. You, D. Ma, *J. Organomet. Chem.* 691 (2006) 3519.
- [9] (a) M. Zhu, J. Zou, X. He, C. Yang, H. Wu, C. Zhong, J. Qin, Y. Cao, *Chem. Mater.* 24 (2011) 174; (b) M. Zhu, Y. Li, S. Hu, C. Li, C. Yang, H. Wu, J. Qin, Y. Cao, *Chem. Commun.* 48 (2012) 2695; (c) M. Zhu, Y. Li, C. Li, C. Zhong, C. Yang, H. Wu, J. Qin, Y. Cao, *J. Mater. Chem.* 22 (2012) 11128; (d) C. Fan, L. Zhu, B. Jiang, Y. Li, F. Zhao, D. Ma, J. Qin, C. Yang, *J. Phys. Chem. C* 117 (2013) 19134; (e) C. Fan, J. Miao, B. Jiang, C. Yang, H. Wu, J. Qin, Y. Cao, *Org. Electron.* 14 (2013) 3392.
- [10] (a) G. Zhou, W.-Y. Wong, B. Yao, Z. Xie, L. Wang, *Angew. Chem., Int. Ed.* 46 (2007) 1149; (b) J. Ding, J. Lü, Y. Cheng, Z. Xie, L. Wang, X. Jing, F. Wang, *Adv. Funct. Mater.* 18 (2008) 2754; (c) G. Zhou, W.-Y. Wong, X. Yang, *Chem. Asian J.* 6 (2011) 1706; (d) S.-C. Lo, N.A.H. Male, J.P.J. Markham, S.W. Magennis, P.L. Burn, O.V. Salata, I.D.W. Samuel, *Adv. Mater.* 14 (2002) 975; (e) S.-C. Lo, P.L. Burn, *Chem. Rev.* 107 (2007) 1097; (f) T. Qin, J. Ding, L. Wang, M. Baumgarten, G. Zhou, K. Müllen, *J. Am. Chem. Soc.* 131 (2009) 14329.
- [11] Y. Shiota, H. Kageyama, *Chem. Rev.* 107 (2007) 953.
- [12] A.L. Von Ruden, L. Cosimbescu, E. Polikarpov, P.K. Koeh, J.S. Swensen, L. Wang, J.T. Darsell, A.B. Padmaperuma, *Chem. Mater.* 22 (2010) 5678.
- [13] N. Miyauro, A. Suzuki, *Chem. Rev.* 95 (1995) 2457.
- [14] A. Tsuboyama, H. Iwawaki, M. Furugori, T. Mukaide, J. Kamatani, S. Igawa, T. Moriyama, S. Miura, T. Takiguchi, S. Okada, M. Hoshino, K. Ueno, *J. Am. Chem. Soc.* 125 (2003) 12971.
- [15] C.-H. Chien, C.-K. Chen, F.-M. Hsu, C.-F. Shu, P.-T. Chou, C.-H. Lai, *Adv. Funct. Mater.* 19 (2009) 560.
- [16] Y. Tao, Q. Wang, C. Yang, C. Zhong, K. Zhang, J. Qin, D. Ma, *Adv. Funct. Mater.* 20 (2010) 304.
- [17] C.-H. Yang, Y.-M. Cheng, Y. Chi, C.-J. Hsu, F.-C. Fang, K.-T. Wong, P.-T. Chou, C.-H. Chang, M.-H. Tsai, C.-C. Wu, *Angew. Chem., Int. Ed.* 46 (2007) 2418.
- [18] W.-Y. Wong, C.-L. Ho, *Coord. Chem. Rev.* 253 (2009) 1709.
- [19] K.A. Knights, S.G. Stevenson, C.P. Shipley, S.-C. Lo, S. Olsen, R.E. Harding, S. Gambino, P.L. Burn, I.D.W. Samuel, *J. Mater. Chem.* 18 (2008) 2121.
- [20] Z.M. Hudson, C. Sun, M.G. Helander, H. Amarné, Z.H. Lu, S. Wang, *Adv. Funct. Mater.* 20 (2010) 3426.
- [21] G. Zhou, C.-L. Ho, W.-Y. Wong, Q. Wang, D. Ma, L. Wang, Z. Lin, T.B. Marder, A. Beeby, *Adv. Funct. Mater.* 18 (2008) 499.
- [22] (a) C.-L. Ho, W.-Y. Wong, G.-J. Zhou, B. Yao, Z. Xie, L. Wang, *Adv. Funct. Mater.* 17 (2007) 2925; (b) R. Wang, D. Liu, R. Zhang, L. Deng, J. Li, *J. Mater. Chem.* 22 (2012) 1411.
- [23] Z. Li, M.-S. Wong, *Org. Lett.* 8 (2006) 1499.
- [24] W.-Y. Lai, Q. He, D. Chen, W. Huang, *Chem. Lett.* 37 (2008) 986.
- [25] (a) K. Noto, Y. Sakai, I. Kakiki, Y. Goto, *PCT Int. Appl.* 2011021385 (2011); (b) S.O. Jeon, J.Y. Lee, *J. Mater. Chem.* 22 (2012) 4233.